Compact 224-Gbit/s Modulator Modules for Digital Coherent Optical Communication Systems

Morihiro SEKI*, Naoya KONO, Takamitsu KITAMURA, Naoki ITABASHI, Taizo TATSUMI and Kazuhiro YAMAJI

Digital coherent technology with multilevel modulation formats is an attractive solution to satisfy the rapid increase in optical traffic demand and has already been adopted in ultra-long haul systems. In the next generation, the application area will be expanded to metro systems, and smaller-sized, lower-power optical components are expected in order to realize high port density. We have developed InP-based modulators and linear driver ICs, which have enabled the modulator module size as small as 34.0 × 16.5 × 6.0 mm^3. We demonstrated that a 224-Gbit/s DP-16QAM modulator module, including all of an InP-based modulator, four linear driver ICs, and polarization multiplexing micro-optics, has comparable performance to $LiNbO_3$-based modulators.

Keywords: digital coherent technology, InP, modulator, linear driver IC, DP-16QAM

1. Introduction

Data communication traffic keeps on increase owing to an evolution of higher-resolution video streaming service and the wide spread of mobile devices, among others. Digital coherent technology with multilevel modulation formats is an attractive solution to satisfy the strong traffic demand and has already been adopted in 100-Gbit/s ultra-long haul systems. In the next generation, the application area will be extended to metropolitan area networks, which require smaller-sized, lower-power optical components to realize higher port density and larger transmission capacity per single port[(1)].

We have demonstrated 128-Gbit/s dual-polarization quadrature phase shift keying (DP-QPSK*[1]) modulators and receivers realized compactness by using InP-based optical devices[(2),(3)]. This paper outlines that a 224-Gbit/s dual-polarization 16-ary quadrature amplitude modulation (DP-16QAM*[2]) modulator module, which includes all of an InP-based modulator, four linear driver ICs, and polarization multiplexing micro-optics, exhibits performance comparable to $LiNbO_3$-based modulators[(4)].

2. Chip Characteristics

2-1 Modulator chip

(1) Design of the modulator chip

Figure 1 (a) shows the top view photograph of the modulator chip. **Figure 1 (b)** shows the cross-sectional view of the modulator section.

Four Mach-Zehnder modulators (MZMs) were monolithically integrated in one modulator chip. The length of the modulator section was 3 mm. A differential S-G-S type electrode configuration was adopted to reduce the area of RF line traces. The differential characteristic impedance of the modulator section was designed to be 90 ohm (Ω).

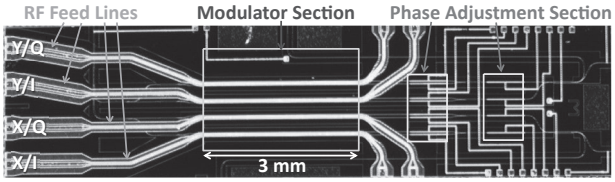

(a) Top view photograph

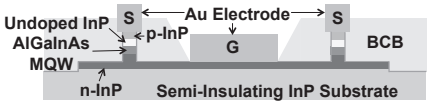

(b) Cross-sectional view of the modulator section

Fig. 1. Modulator chip

We used deep-ridge optical waveguides because of the advantages of compact routing of light and low capacitance between S-G electrodes[(5)]. The width and height of the waveguides were 1.6 μm and 3 μm respectively. The core material of the waveguides was undoped AlGaInAs multi quantum wells (MQWs), which led to higher modulation efficiency that was a large index change with low optical loss at a high bias voltage. The waveguides were buried with a thick benzocyclobutene (BCB) layer in the modulator section to feed RF transmission lines.

(2) Characteristics of the modulator chip

Figure 2 shows the measured waveguide width dependence of optical propagation loss. The propagation loss for 1.6-μm width waveguides was less than 0.25 dB/mm over the C band. This result indicates that scattering loss at the sidewall of fabricated deep-ridge waveguides and absorption loss were suppressed adequately.

Figure 3 shows the optical loss increase due to the

reverse bias voltage applied to the modulator section. The loss increase was less than 1 dB, even with high voltages of up to 11 V at a wavelength of 1570 nm.

Figure 4 shows the typical DC extinction characteristic for a wavelength of 1570 nm. We obtained a DC extinction ratio (ER) of more than 25 dB with a reverse bias voltage of 11 V.

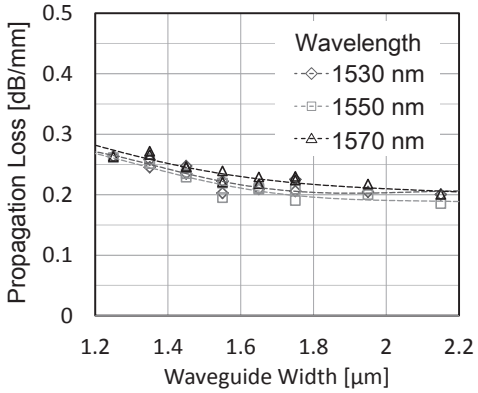

Fig. 2. Waveguide width dependence of optical propagation loss

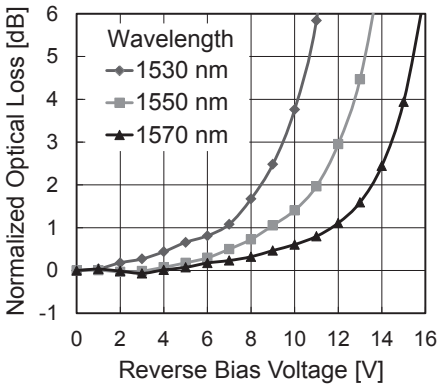

Fig. 3. Reverse bias voltage dependence of optical loss increase

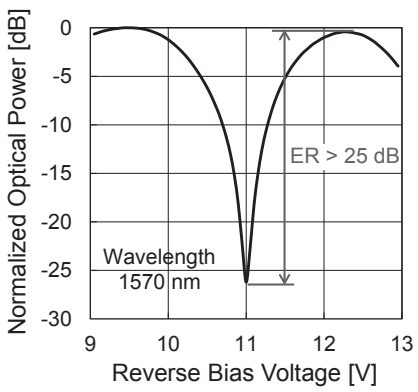

Fig. 4. Typical DC extinction ratio

2-2 Linear driver IC

(1) Design of the linear driver IC

Figure 5 shows the block diagram of the linear driver IC. We adopted a traveling wave amplifier (TWA)[6] to achieve both a high-speed operation and low return losses. The TWA stage consisted of 6 distributed linear amplifier unit cells and coplanar lines, and differential 90-ohm output termination. A single TWA stage configuration allowed for a high linearity with low power dissipation.

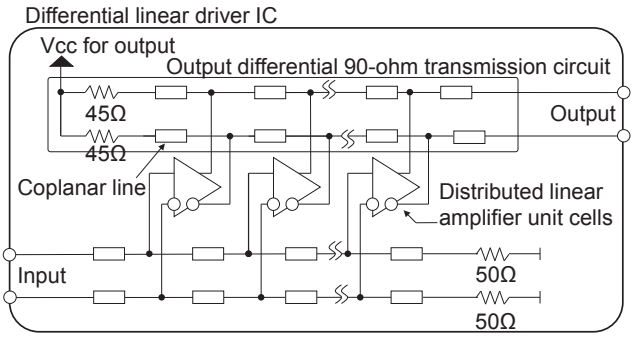

Fig. 5. Block diagram of the linear driver IC

We added a gradual frequency peaking to Sdd21 of the linear driver IC to compensate for RF losses in the module.

The typical differential output voltage swing of the driver IC was 2.5 Vpp. We calibrated the above mentioned modulator so that the output voltage swing of the driver IC would correspond to 1.0 Vπ. Although this driving condition of 1.0 Vπ decreased the peak optical output power by 3 dB, compared with the condition of 2.0 Vπ, this under-drive modulation could save the power dissipation of the ICs, eliminate inductors for DC biasing, and reduce a nonlinear distortion of a sinusoidal optical field response of the modulator.

The chip size of one IC was 1.1 × 2.1 mm^2, and total assembly area for four ICs was only 9.0 × 2.1 mm^2 thanks to the inductor-less design. The driver IC was fabricated with an InP double heterojunction bipolar transistor (DHBT) technology with a maximum cut-off frequency (ft) of 150 GHz and a maximum oscillation frequency (fmax) of 200 GHz.

(2) Characteristics of the linear driver IC

Figure 6 (a) shows measured s-parameters. Both Sdd11 and Sdd22 were below -10 dB up to 50 GHz. A 3-dB cut off frequency of Sdd21 reached 45 GHz. A gradual peaking of Sdd21 from 3 GHz to 28 GHz compensated for RF losses of the modulator module.

Figure 6 (b) shows the total harmonic distortion (THD) of 1 GHz sinusoidal wave input as a function of the differential output voltage. THD was around 2.5 percent (%) even at the differential output voltage of 2.5 Vpp.

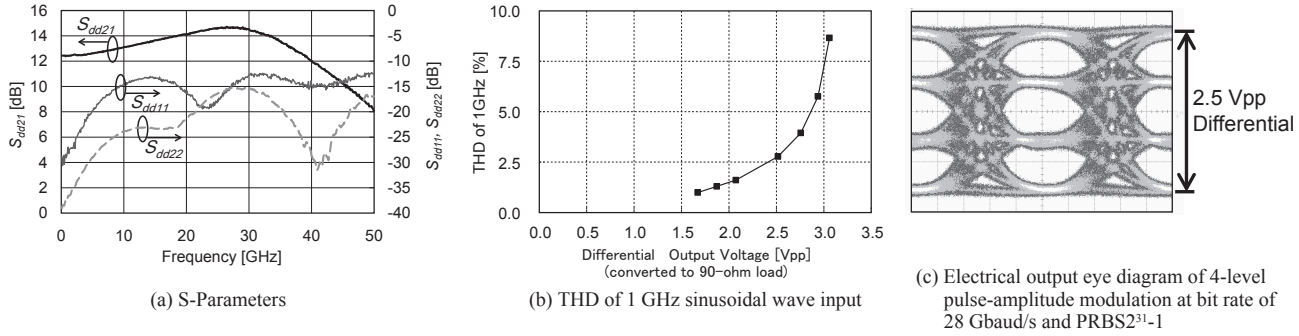

(a) S-Parameters

(b) THD of 1 GHz sinusoidal wave input

(c) Electrical output eye diagram of 4-level pulse-amplitude modulation at bit rate of 28 Gbaud/s and PRBS2[31]-1

Fig. 6. Measurement results of the linear driver IC

Figure 6 (c) shows an electrical output eye diagram with 28-Gbaud/s 4-level amplitude modulation. In this case, the differential input voltage swing was 650 mVpp, which can be supplied by the digital-to-analog converter (DAC) directly. The differential output voltage swing was 2.5 Vpp. Clear 4-level eye openings were observed.

3. Characteristics of the Modulator Module

Photo 1 and Figure 7 show an appearance of the modulator module and a block diagram of the modulator module respectively. The modulator module included all of an InP-based modulator chip monolithically integrating four MZMs, four linear driver ICs, polarization multiplexing micro-optics, and thermo-electric cooler (TEC) for the modulator chip and the micro-optics. To minimize the package size, we located the input and output fibers on the same side of the package and RF interfaces on the opposite side. The modulator module size was only 34.0 × 16.5 × 6.0 mm^3.

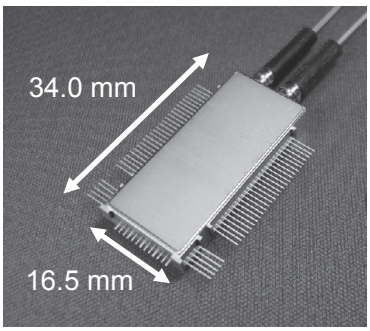

Photo 1. Appearance of the modulator module

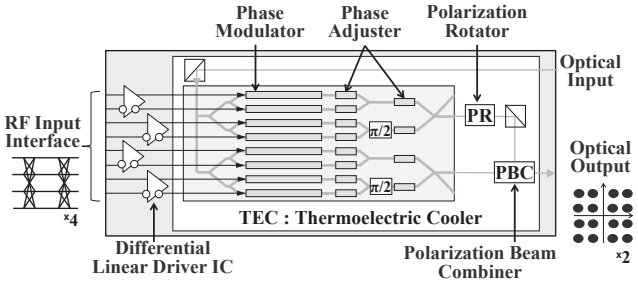

Fig. 7. Block diagram of the modulator module

Figure 8 (a) and (b) show small-signal E/O response and Sdd11 of each channel of modulators respectively. There were two dips around 17.5 GHz and 21 GHz in E/O response due to relatively high Sdd11 caused by mismatch losses at RF input interfaces. Ignoring these mismatch losses, a 3-dB cut-off frequency of this module was around 20 GHz.

Figure 9 shows experimental results of single polarization (SP)-16QAM operation for both 14 Gbaud/s and 28 Gbaud/s. **Figure 9 (a) and (b)** show the back-to-back bit error rate (BER) as a function of optical signal-to-noise ratio (OSNR). **Figure 9 (c) and (d)** show the sample recovered 16QAM constellations*3 of this work. In this experimental setup, tunable lasers with linewidth of about 500 kHz were used, and a 50-Gsamples/s oscilloscope was used to digitize the electrical outputs of a coherent receiver. Results of $LiNbO_3$-based modulator, a 3-dB bandwidth was over 22 GHz, measured in the same experimental setup and theory lines[7] are also plotted for a comparison in **Fig. 9 (a) and (b)**. In these results, the difference between this work and $LiNbO_3$-based modulator was small. At 10^{-3} of BER curves, the deviations of this work from theoretically expected values were within 2.8 dB for 14 Gbaud/s and 5.6 dB for 28 Gbaud/s.

The power dissipation of this module was lower than 3.2 W, of which 2.4 W were for the four driver ICs and 0.8 W for the TEC.

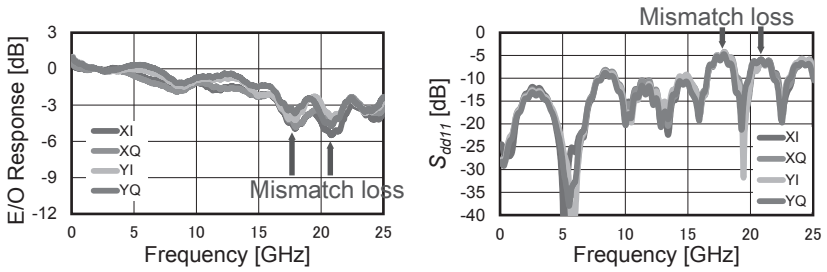

(a) E/O response (b) Sdd11

Fig. 8. Measured small-signal frequency response of DP-16QAM module

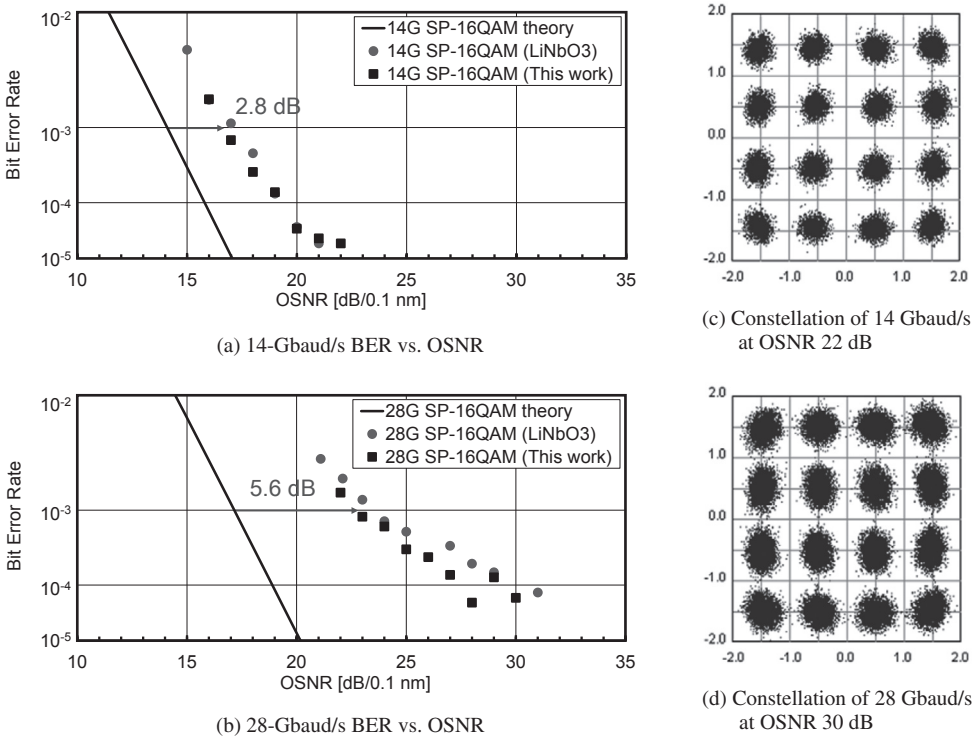

(a) 14-Gbaud/s BER vs. OSNR

(b) 28-Gbaud/s BER vs. OSNR

(c) Constellation of 14 Gbaud/s at OSNR 22 dB

(d) Constellation of 28 Gbaud/s at OSNR 30 dB

Fig. 9. Experimental results of SP-16QAM operation

4. Conclusion

We developed InP-based modulators and linear driver ICs, which enabled a compact and low-power modulator module. The size of the modulator module, including all of an InP-based modulator, four linear driver ICs, and polarization multiplexing micro-optics, was just 34.0 × 16.5 × 6.0 mm^3. We demonstrated that a 224-Gbit/s DP-16QAM modulator module has performance comparable to $LiNbO_3$-based modulators.

Technical Terms

∗1 DP-QPSK: Dual-Polarization (DP) Quadrature Phase Shift Keying (QPSK). QPSK is a modulation method that uses four phase states, which are different by 90 degrees in each.

∗2 16QAM: 16-ary Quadrature Amplitude Modulation. 16QAM is a modulation method that combines two carriers whose phases are different by 90 degrees and whose amplitudes are modulated into four levels independently. One modulated signal can represent 16 states on a complex plane. With DP-16QAM, 8-bit data can be transmitted in one time slot.

∗3 Constellation: A figure which expresses the phase and amplitude of data signals on a complex plane.

References

(1) W. Forysiak, "Progress in InP-based Photonic Components and Sub-systems for Digital Coherent Systems at 100 Gbit/s and beyond," ECOC13, Mo.3.C.2 (2013)

(2) N. Kono et al., "Compact and Low Power DP-QPSK Modulator Module with InP-Based Modulator and Driver ICs," OFC/NFOEC2013, OW1G.2.

(3) H. Yagi et al., "High-Efficient InP-Based Balanced Photodiodes Integrated with 90˚ Hybrid MMI for Compact 100 Gb/s Coherent Receiver," OFC/NFOEC2013, OW3J.5.

(4) T. Tatsumi et al., "A Compact Low-Power 224-Gb/s DP-16QAM Modulator Module with InP-based Modulator and Linear Driver ICs," OFC/NFOEC 2014, Tu3H.5.

(5) H. Yagi et al., "Low Driving Voltage InP-Based Mach-Zehnder Modulators for Compact 128 Gb/s DP-QPSK Module," in Conf. on Lasers and Electro-Optics Pacific Rim, and OptoElectronics and Commun. Conf./Photonics in Switching (CLEO-PR&OECC/PS), WK2-1 (July 2013)

(6) Y. Baeyens et al., "High Gain-Bandwidth Differential Distributed InP D-HBT Driver Amplifiers With Large (11.3Vpp) Output Swing at 40Gb/s," IEEE JOURNAL OF SOLID-STATE CIRCUITS, VOL. 39, NO. 10 (OCT. 2004)

(7) K. Kikuchi, and S. Tsukamoto, "Evaluation of Sensitivity of the Digital Coherent Receiver," JOURNAL OF LIGHTWAVE TECHNOLOGY, VOL. 26, NO. 13 (JULY 1, 2008)

Contributors (The lead author is indicated by an asterisk (*).)

M. SEKI*

- Assistant General Manager, Transmission Devices R&D Laboratories

N. KONO

- Dr. Information Science
  Assistant Manager, Transmission Devices R&D Laboratories

T. KITAMURA

- Transmission Devices R&D Laboratories

N. ITABASHI

- Transmission Devices R&D Laboratories

T. TATSUMI

- Assistant General Manager, Transmission Devices R&D Laboratories

K. YAMAJI

- Assistant General Manager, Transmission Devices R&D Laboratories